Modelling of induction heating in steel reheating furnaces

Ted Sjöberg[1], Gustav Häggström[1], Mattias Gärdsback[2], Stefan Marth[1]
1. Swerim AB, Luleå, Sweden
2. Alleima, Sandviken, Sweden.

Abstract

Today reheating furnaces in the steel industry are commonly heated by combustion of fossil fuels. Induction heating is one possible way on the transition towards a carbon free steel industry. To support the change from furnaces with fossil energy towards alternative heating furnaces, modelling and simulation has an important role in decision making and design of new furnaces. In this paper a method to use COMSOL Multiphysics to simulate induction reheating are presented, and the simulation results are then compared and validated against pilot trials performed at Swerims pilot facility in Luleå.

Two steel grades were evaluated: one low-alloyed ferritic carbon steel, and one stainless ferritic-austenitic Super Duplex 2507 steel. The workpieces had rectangular cross-sections of 290x125 mm and lengths of 1700mm for both steel grades. The validation experiments were conducted at the pilot facility using a 900kW induction heater with 4 coils. The workpieces were heated using a frequency of 350 Hz from room temperature to 1200 degrees Celsius in the centre of the workpiece. The temperature was measured during the experiments using five thermocouples at different positions inside the workpiece. The temperature history, the electrical power input and the cooling losses were later used for validation of the modelling results.

A model of the pilot induction furnace was set-up using COMSOL Multiphysics in which the full resonant circuit of the furnace was modelled using a coupled electrical circuit. The coils of the furnace were modelled using the numeric multi-turn coil feature to make it possible to use quarter symmetry of the furnace using only 250 000 elements in the mesh. Movement of the workpieces through the coils was modelled with a deforming mesh, while the induction heating itself was modelled using the Multiphysics interface "Electromagnetic Heating" to couple the magnetic fields and temperature in the workpieces. The electromagnetic heating was modelled using a simplified approach in which only the effects of eddy-currents were considered, and the hysteresis of the material was ignored.

The results show that the reheating of steel workpieces with induction can be modelled using COMSOL Multiphysics. Comparisons with experimental results from Swerim's pilot plant show reasonable agreement even when using a simplified model. This first model show that, with some further development and modifications, COMSOL Multiphysics can be very useful for modelling existing and future reheating furnaces in order to support the industry in the transition from carbon based reheating furnaces to electrical heating furnaces and therefore contribute towards a fossil-free steel industry.

Keywords: Induction furnace modelling, experimental validation.

Introduction

As industry today is decreasing fossil-fuel dependency one area of focus is the reheating of metal workpieces. One process of heating metal directly using electricity is by utilising induction heating. Heating through induction is achieved by alternating a magnetic field around the metal workpiece, leading to an induced current inside the workpiece. This eddy current will result in heating of the workpiece through Joule heating, which is commonly the largest contributing factor in the induction heating process. In magnetic materials heat is also generated by hysteresis losses.

Induction heating is a non-contact heating method in which the heat is generated within the workpiece itself. This makes it possible to achieve very rapid temperature increase, as the process is not dependent on external heat transfer.

Modelling of induction heating is a complex problem, involving the time-consuming task of solving Maxwell's equations for electromagnetic fields coupled with energy equations for the heat transfer in the workpiece. COMSOL Multiphysics is a FEM software that has been used to simulate a wide range of different induction applications such as electromagnetic stirring [1] and advanced heating systems [2]. Adding to the complexity of modelling induction heating is the inherent non-linearity of the problem due to the many temperature-dependent material properties of the workpiece, requiring extensive testing for multiple material parameters at several temperatures.

One such temperature dependent parameter is the magnetic response. To model the magnetic constitutive relation within a steel workpiece there exists many different approaches, as an example Mörée and Leijon [3] has performed a review of the most commonly used models. Magnetic constitutive models vary significantly in complexity, and consequently in areas such as material testing needed to calibrate the model and computational cost. It should be noted that while some of the models reviewed come pre-implemented into modelling software such as COMSOL Multiphysics, some models require significant work to successfully implement.

Experimental setup

The induction furnace consisted of four identical longitudinal coil packs, connected in series, with a hydraulically reversible roller track to feed workpieces through the furnace. Both coil packs and roller track are cooled with a continuous flow of water, with temperatures and flows measured. At the ends of the coils, two insulating hoods were mounted around the roller track to preserve the heat in the workpieces as they were oscillated back and forth in the furnace. The maximum power available was 900 kW, actual power depending on dimensions and magnetic properties of the material. To regulate the power, the voltage and frequency of the alternating current was varied. The voltage was regulated directly through the furnace control system, continuously between 0-2200 V. The frequency could be set stepwise between 350 and 600 Hz by varying the size of a capacitor bank that creates a resonant circuit together with the coils. The speed of the roller track could be varied between 10–100 mm/s in the furnace control system. The coils of the furnace were rectangular and fit workpieces with a maximum cross-sectional area of 300*125 mm. The furnace was ceramically lined and partially enclosed from the surroundings. Both ends of the furnace, as well as gaps for the roller track on the sides of the furnace, were open for gas exchange with the surroundings, which leads to radiation and convective heat losses. During the experiments, temperatures were logged using pyrometers and a thermal camera directed into the furnace onto the side faces of the workpieces. With the thermal camera, the sides of the workpieces were scanned to produce images showing the development of the temperature distribution during the heating process. Data from the cooling water for induction coils was logged, with flow and temperature sensors on both incoming and outgoing water.

During all experiments, workpiece temperatures were also monitored using embedded thermocouples. For each workpiece five thermocouples were mounted, Figure 1. All thermocouples were placed in the centre of the steel workpieces as seen from the end face.
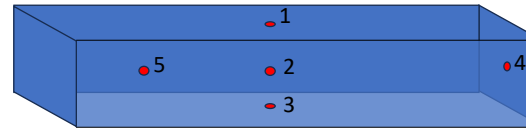

Figure 1. Positioning of thermocouples
1 – Top of workpiece, 10 mm below surface
2 – Centre of workpiece
3 – Bottom of workpiece, 10 mm below surface
4 – End of workpiece, centred, 50 mm below surface
5 – Quarter of workpiece length, centred

Geometry

Full field 3D-simulations of an induction heating process of steel workpieces were performed using COMSOL Multiphysics. As the induction furnace coils and heated workpieces had rectangular cross-sections an axisymmetric model could not be utilized. However, using planar symmetry only a quarter of the geometry was modelled and thereby the computational cost was minimized. The model consisted of four coil packages where each coil package consisted of a pair of coils with opposing coil directions. Each coil in the pairs is slightly shorter than 250 mm, making one coil package slightly longer than half a meter. The packages are spaced with roughly 300 mm distance in between, making the furnace close to three meters in length. The coils have a width of 430 mm and a height of 230 mm. The steel workpieces modelled are 1680 mm long and has a cross-section of 265 by 120 mm. The workpiece is oscillating back and forth inside the furnace to get a more even heat distribution. To enable modelling of this oscillating motion the air domain is split into two parts. One
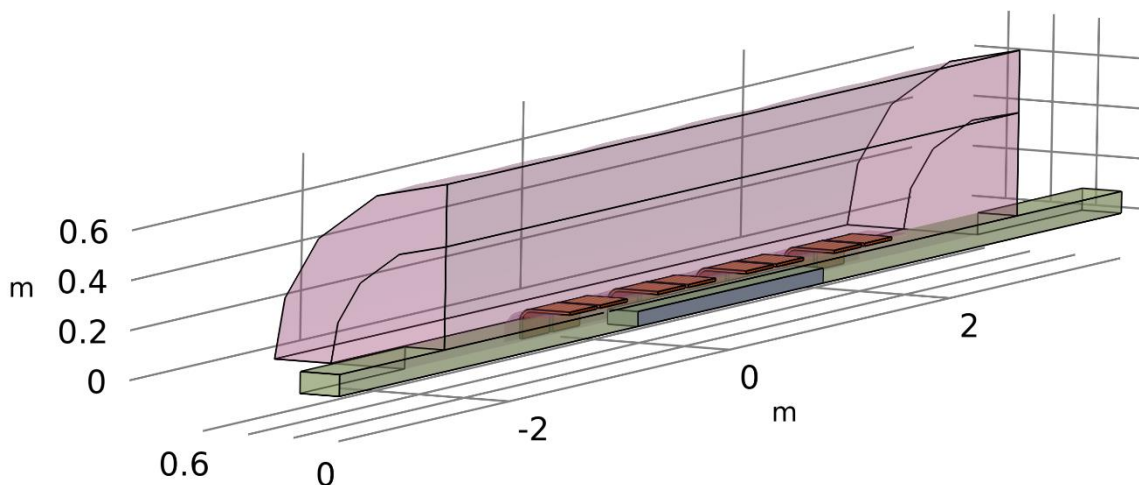

Figure 2. Model geometry overview, showing the cylindrical stationary air domain shaded in red, and the smaller moving air domain shaded green. The four coil package pairs are coloured orange and the steel bloom grey.

2

large domain modelled as a cylinder encapsulating the entire furnace, and one smaller domain that only encompass parts of the air inside the induction coils. This smaller air domain follows the workpieces motion, making it possible to use a non-deforming mesh throughout the simulation. The moving air domain was also extended outside the cylindrical part of the larger air domain so that there is never any gap formed in the main domain throughout the movement of the workpiece. An overview of the model is shown in Figure 2.

Governing Equations

The model is built from two main physics interfaces, "Magnetic Fields" and "Heat transfer in solids". These interfaces are then linked together using the "Electromagnetic heating" Multiphysics interface [4]. In addition, the electric circuit of the furnace is modelled using the "Electronic circuit" interface. To minimize the impact of the boundary conditions far from the workpiece an infinite element domain was applied on the cylindrical air domain. The infinite element domain adds a scaling to the domain, effectively putting the boundary further away without needing to model a larger domain.

Magnetic fields

The magnetic fields interface in COMSOL were used in a frequency domain study to calculate the electromagnetic fields ($\boldsymbol{E}, \boldsymbol{B}$) from the Maxwell equations using the vector potential $\boldsymbol{A}$

$$\nabla \times \boldsymbol{H} = \boldsymbol{J}$$
$$\boldsymbol{B} = \nabla \times \boldsymbol{A}$$
$$\boldsymbol{E} = -j\omega\boldsymbol{A}$$
$$\boldsymbol{J} = \sigma\boldsymbol{E} + j\omega\boldsymbol{D}$$

The main node in this interface is the Ampère's law which provides an interface for defining constitutive relations as well as electric properties for the used materials. Two nodes of Ampère's law were defined, one for the air domains and one for the steel workpiece.

For the simulations in this paper, the constitutive relation between the magnetic flux density $\boldsymbol{B}$ and the magnetic field $\boldsymbol{H}$ was based on a relative permeability relation,

$$\boldsymbol{B} = \mu_0\mu_r\boldsymbol{H}$$

in which the relative permeability was described by a dependency on the strength of the magnetic flux density norm and the temperature in the material. The relative permeability is described by

$$\mu_r = \left(C_1 + C_2 e^{C_3|\boldsymbol{B}|} + C_4 e^{C_5|\boldsymbol{B}|}\right)\left(1 - \left(\frac{T}{T_C}\right)^6\right)$$

where C_x is material dependent constants and T_C is the Curie temperature of the material. This is a simple model that unfortunately has the drawback of not being able to model hysteresis or magnetic remanence. However, Super Duplex 2507 is a soft magnetic model making this simplification applicable. The material parameters for the Super Duplex steel were calibrated from data given in [5].

For the ferritic steel, the dependency on the magnetic flux density was assumed to be negligible and parameters $C_2 - C_5$ was set to zero. The room temperature permeability of the carbon steel was set as $C_1 = 800$, while the Curie temperature was approximated to 780°C.

The conduction model used was a simple electrical conductivity, where the workpiece electrical conductivity was temperature dependent. For the Super Duplex steel the conductivity was input as a piecewise linear dependency with values taken from MatWeb [6] while for the low alloyed carbon steel the conductivity used a temperature and carbon content dependent model described by Yafei et al [7].

$$\sigma = \frac{1}{\rho} = (0.065 + 0.474 * 10^{-3}T + 0.889$$
$$* 10^{-6}T^2 + 0.122 * C^{0.25})^{-1}$$

where T is the temperature and C is the carbon content of the steel, in this case assumed to be 0.13%.

For all simulations a dielectric model was used where the relative permittivity of the material was set constant at a value of unity.

The coils of the induction furnace were defined as homogenized multiturn conductors with 8 turns each, where every second coil were defined as having the current flow in the reverse direction. The coil excitation of the coils was calculated by connecting the coils to an "External U vs I" in an Electrical circuit interface as explained further in a later section of this paper.

To obtain convergence in the simulation even using a linear discretization of the magnetic vector potential, a gauge fixing for the A-field was used.

Heat transfer in solids

To simplify the modelling only the steel workpiece is taken into consideration in the energy equations. The air and coils are assumed to have constant temperature and to not impact the heat transfer in the workpiece. To enable the use of quadratic symmetry the conveyors beneath the workpiece are ignored, and the workpiece is assumed to only be surrounded by air. The workpiece is modelled by the standard heat transfer in solids node, defined by the equation

$$\rho C_p \frac{\partial T}{\partial t} + \rho C_p \boldsymbol{u} \cdot \nabla T + \nabla \cdot \boldsymbol{q} = Q$$
$$\boldsymbol{q} = -k\nabla T$$

Since the workpiece is solid, and thereby not moving in the material frame, the velocity field **u** is zero. The heat sources, Q, in the right-hand side of the equation are implemented through the multiphysics coupling. The electromagnetic losses from the magnetic fields node are included as a heat source in the energy equation. The boundaries of the workpiece, disregarding the symmetric boundaries, have two sources of heat loss: radiation and convection. The surface-to-ambient radiation is calculated as

$$-\boldsymbol{n} \cdot \boldsymbol{q} = \varepsilon\sigma(T_{amb}^4 - T^4)$$
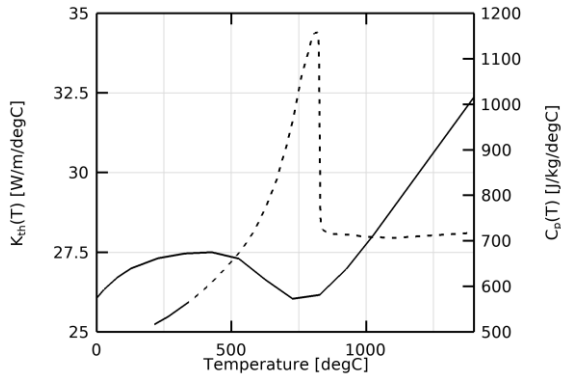
Figure 3. Thermal properties of carbon steel. Thermal conductivity in solid line on left hand axis, specific heat in dashed line on righthand axis.

where the surface emissivity ε is set to a constant 0.7 as the temperature dependency of the emissivity for the used steel is unknown, and the ambient temperature is set to slowly increase to 450°C to roughly model the elevated temperatures within the half open induction furnace. The convective heat flux is calculated as

$$-\boldsymbol{n} \cdot \boldsymbol{q} = h(T_{amb} - T)$$

where the heat transfer coefficient h is set to 5 [W/m²/K].

For the Super Duplex steel material data for the energy equations were taken from literature. Taieh et al. [8] found that Mills equations [9] for Stainless steel 300 series are good approximations also for Super Duplex 2507. The temperature dependent relations given by Mills for 300 series stainless steel used in this model was the specific heat capacity $\left[\frac{J}{kg\ K}\right]$

$$C_p = 472 + 13.6 * 10^{-2} * T - 2.82 * 10^6 / T^2$$

and for the thermal conductivity $\left[\frac{W}{m\ K}\right]$

$$k_{th} = 9.2 + 0.0175 * T - 2 * 10^{-6} * T^2$$

The density was assumed to be constant, since thermal expansion was neglected, with a value of

$$\rho = 7800 \frac{kg}{m^3}$$

For the simulation of the carbon steel the specific heat and thermal conductivity was modelled using

linear piecewise tabulated data from Figure 3. the Curie temperature was assumed to be 780°C, and the density was assumed to be the same as for the Super Duplex steel.

Electrical circuit

To model the controlling LC-circuit of the induction furnace an "Electrical circuit" interface was added to the model. The interface modelled the voltage of the furnace using a voltage source and the capacitor bank using a single simple capacitor with a capacitance of 440 μF. The eight coils of the durance were modelled individually according to the scheme in Figure 4, and each coil was modelled as external current sources coupled to the currents running through the coils in the magnetic fields interface. Using this setup, it was possible to calculate the individual voltage drop of each coil as the workpiece oscillated.

Furthermore, the electrical circuit node was used in preliminary simulations to verify that the resonant frequency for the model was close to the value measured in the experiments. The resonant frequency was determined to be close to 350 Hz, which was the target frequency of the experimental trials. This was also the frequency used in the frequency-transient simulation.
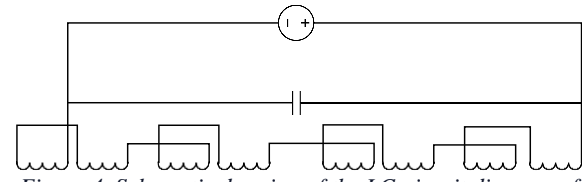

Figure 4. Schematic drawing of the LC-circuit diagram of the induction furnace.

Moving workpiece

To enable motion of the workpiece while retaining continuity, especially of the curl of the vector fields, one needs to be careful when choosing what approach to use. For the model described here an approach of discrete stepping while maintaining mesh continuity was utilized. As described earlier the geometry was split into two regions, one static region containing the induction coils and a larger
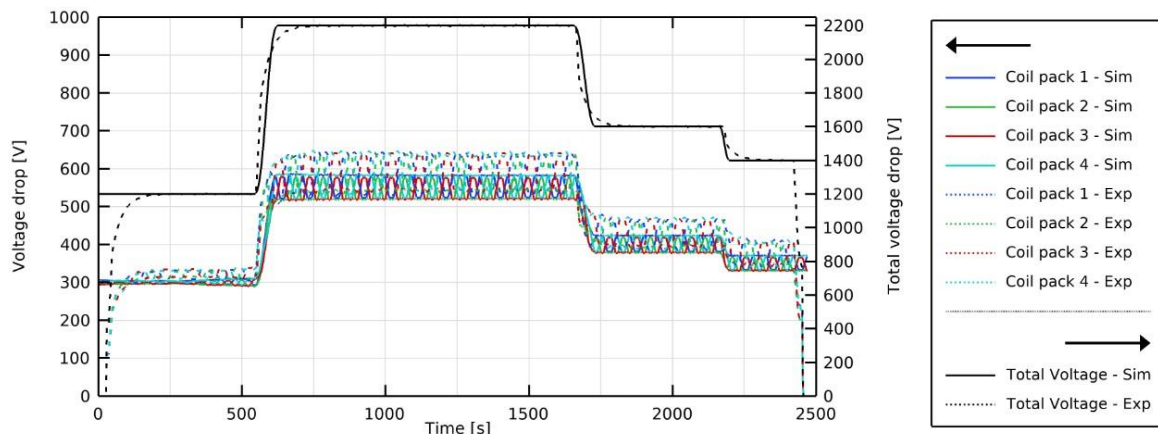

Figure 5 Comparison for Super Duplex 2507 case of voltage drop over the four coil packs plotted in colour Righthand axis show total voltage drop for plots in black.
Dashed lines show results from experiment and solid lines from simulation.
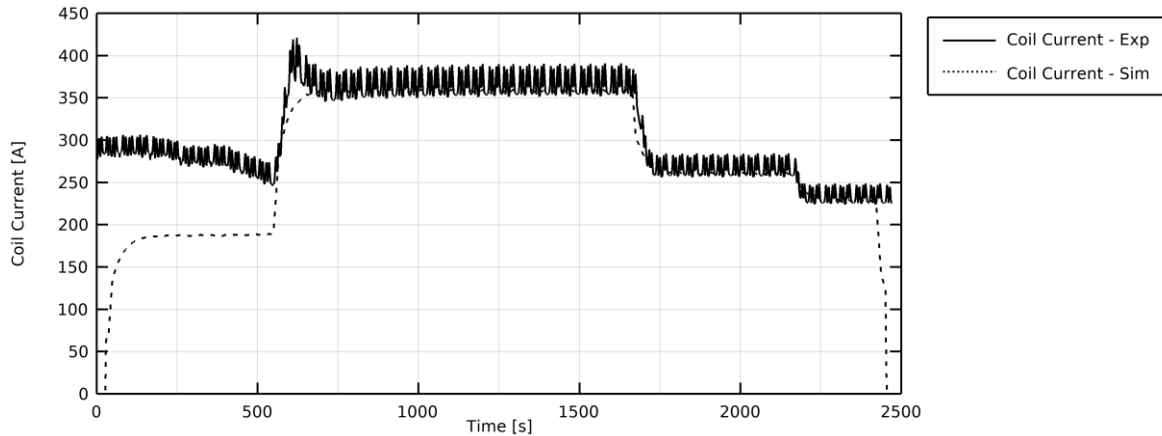
Figure 6. Comparison of current running through the induction coils for the Super Duplex 2507 case.
Dashed lines are experiment; solid lines are simulation.

region of air, and the other containing the moving workpiece and a small region of surrounding air. The contact area between these two regions is defined as an identity boundary pair that is divided into small subsections with identical area and meshes. Then, it is possible to step forward the moving region exactly the length of one subsection and end up with the mesh still perfectly aligned. The movement of the workpiece is triggered in the solver by using events to trigger a prescribed motion of the mesh. The velocity of the workpiece is controlled by the trigger frequency of the event and the size of the subsections. The velocity of the rollers in the experimental trials was 40 mm/s for the Super Duplex steel and 20 mm/s for the carbon steel. These velocities were obtained by taking 50 mm steps every 1.25 or 2.5 seconds respectively. The time-stepping of the simulations was also limited to ensure that there was at least one time-step for each movement step.

Results and Discussion

The model of the LC-circuit is relatively accurate for the Super Duplex 2507, Figures 5-7. The voltage drop across the induction coils is shown in Figure 5. The total voltage drop is an input parameter for the simulations. Except for the

starting and end voltage not being zero the simplified total voltage curve of the simulation follows the experimental measurement well. The resulting voltage drop across the individual coil packs is an output of the electrical circuit calculations. One observation is that the model underpredicts the maximum voltage of the coil packages by almost 10% and the lowest voltage by roughly 5%, even though the total voltage is input at the exact measured level. This is most probably an effect of model simplifications such as ignoring all electrical losses in cables and the capacitor bank. Another source of error is the assumption of the AC current having a sinusoidal shape, which is required for the used frequency domain simulations. However, the experimental induction furnace uses a thyristor-based current feed system that will output a slightly deformed waveform.

Looking at the current running through the induction coils, shown in Figure 6 the simulation overpredict the current by roughly 100 Ampere for the first 500 seconds while agreement is good the rest of the time.

For the power running through the induction coils, Figure 7, the agreement between experimental and simulated results is good. While both the low and high values of the power output are slightly lower
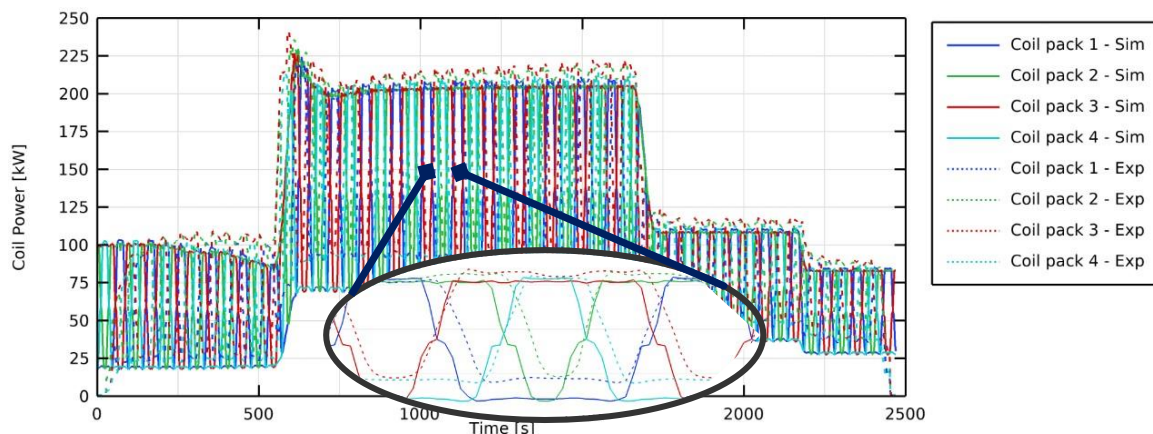

Figure 7. Comparison of power of the induction coils in the Super Duplex 2507 case.
Dashed lines are experiment; solid lines are simulation.
Zoomed in section shows one cycle of the bloom at maximum power.
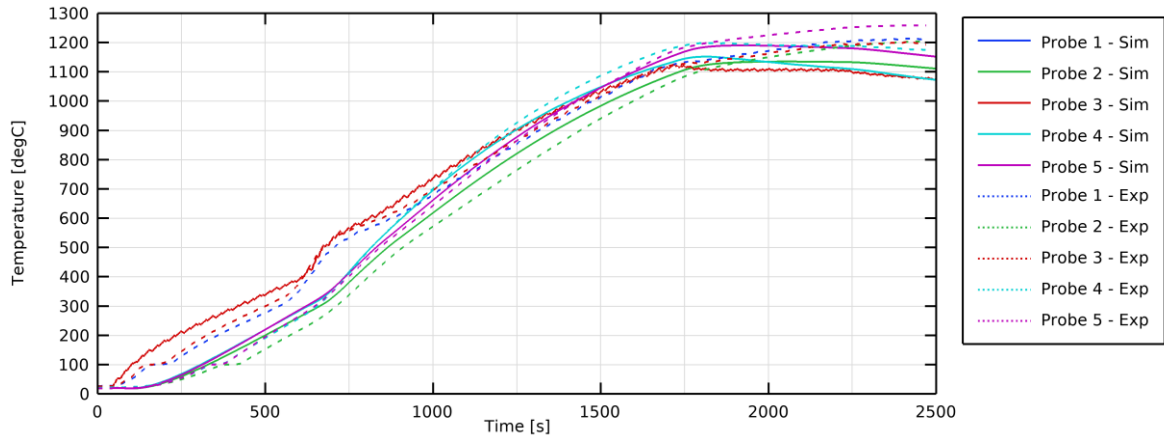
5

Figure 8. Comparison of temperature within the Super Duplex 2507 workpiece at the given thermocouple positions. Dotted lines are experiment; solid lines are simulation.

in the simulation, the overall agreement is satisfactory. Since the coil power is what will govern the heating characteristics of the induction furnace, this is the most important variable. The temperature was measured using thermocouples at five positions in the workpiece, Figure 1. Since quarter symmetry was used, the model gave identical results for the temperatures at thermocouples 1 and 3, Figure 8. The temperatures at thermocouples 1 and 3 show good agreement at the start of the heating process. At 550°C there is a decline in heating rate, which is the result of reaching the Curie temperature of the material. The similarity of the temperature history indicates that both the power-law magnetic flux density dependency and the simple temperature dependency are reasonable approximations of the material response. At the end of the heating cycle there is a period of soaking where the applied power is decreased. During this period the temperature continued to increase in the trials, while it decreased in the simulation. One probable reason for this discrepancy is that the boundary conditions in the energy equations are not accurate enough. The simple assumption of a constant surrounding

temperature with a small fixed forced convection loss is not enough to accurately model the losses of the workpiece over the entire heating period. The results from the simulation of the low carbon steel are shown in Figure 9 and Figure 10. Figure 9 shows both the total voltage drop over all coils and the individual voltage drop over the four coil packages. The total voltage curve for the experiments is not as smooth as the idealised voltage curve used in the simulations. Also, the power drop over the individual coil packages are underpredicted somewhat in the simulation, similarly as for the previous steel grade. The temperature history at the positions of the thermocouples is different in the beginning of the experiments compared to the simulations, Figure 10. The heating in the experiment is more rapid in all measured positions of the workpiece. Once the temperature exceeds the Curie point after 400 seconds, the experiment and simulation show much better agreement. This is partly because the increase in voltage occurs earlier in the experiment than the simulation. For the low carbon steel, the assumed material model is not accurate enough, and better material data may improve the results.
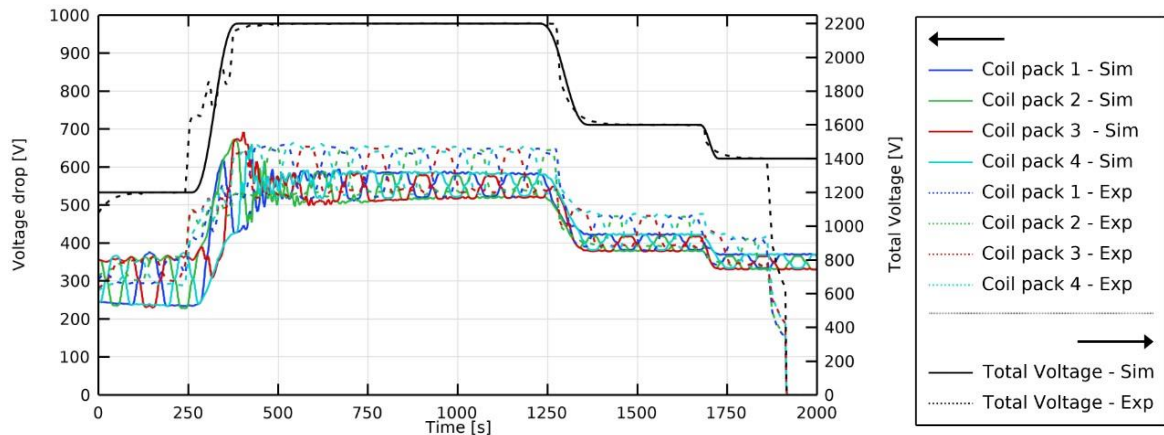

Figure 9. Comparison of voltage drop over the four coil packs for carbon steel plotted in colour
Righthand axis show total voltage drop for plots in black.
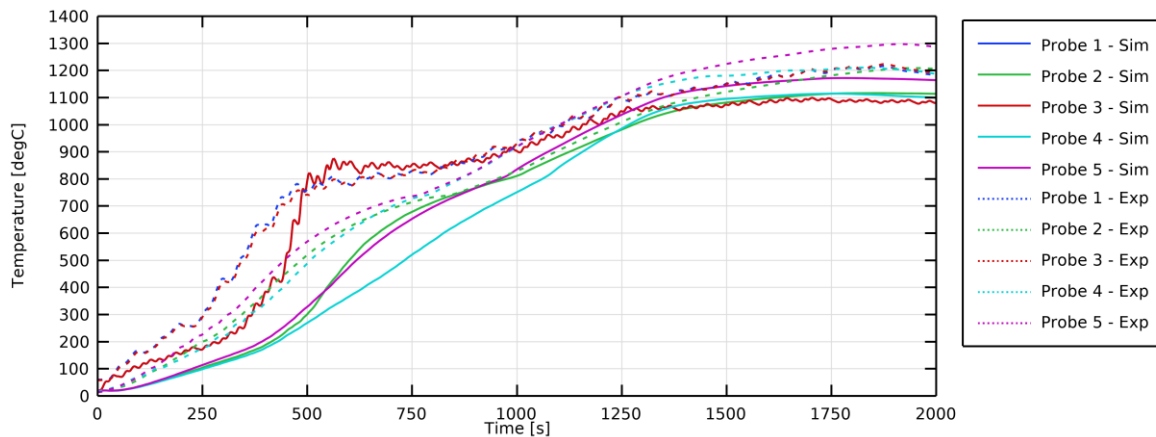*Dotted lines show results from experiment and solid lines from simulation.*

Figure 10. Comparison of temperature within the carbon steel workpiece at the given thermocouple positions. Dotted lines are experiment; solid lines are simulation.

Just as for the Super Duplex steel the temperature difference between experiment and model increases in the last part of the heating. Again, this discrepancy is most likely due to the simple boundary conditions used for the heat transfer.

Conclusions

In this paper a simulation model for induction heating of steel workpieces is validated against results from pilot plant experiments. The heating history of the workpiece is captured in several positions by inserted thermocouples and used in the validation of the model. Comparison of the results show that the model can predict the overall heating characteristics of the induction furnace for Super Duplex 2507 steel. However, further work on refining the material model for low carbon steel is needed, where improvements of model behaviour at temperatures below Curie temperature may lead to improved prediction of the heating rate at the beginning of the process. For both materials more accurate boundary conditions, with focus on the thermal boundary conditions, may give significant improvements in the performance of the model. Improving the radiation and convection on the boundary of the workpiece will most probably make it possible to predict the final temperature of the workpiece more accurately.

References

[1] C. Mapelli, A. Gruttadauria and M. Peroni, "Application of electromagnetic stirring for the homogenization of aluminium billet cast in a semi-continuous machine," *Journal of Materials Processing Technology,* pp. 306-314, 2010.

[2] I. Iatcheva, I. Lilyanova, H. Tahrilov and R. D. Stancheva, "Industrial Heating System Creating Given Temperature Distribution," *Serbian Journal of Electrical Engineering,* vol. 5, no. 1, pp. 57-66, 2008.

[3] G. Mörée and M. Leijon, "Review of Hysteresis Models for Magnetic Materials," *Energies,* vol. 16, no. 9, 2023.

[4] COMSOL Multiphysics Reference Manual, COMSOL.

[5] M. Fisk, "Modelling of Induction Heat Treatment in a Manufacturing Chain," Universitetstryckeriet, Luleå, 2011.

[6] "MatWeb," Matweb LLC, [Online]. Available: www.matweb.com. [Accessed 05 2023].

[7] S. Yafei, N. Dongjie and S. Jing, "Temperature and Carbon Content Dependence of Electrical Resistivity of Carbon Steel," in *4th IEEE Conference on Industrial Electronics and Applications*, Xi'an, 2009.

[8] K. C. Mills, Y. Su, Z. Li and R. F. Brooks, "Equations for the Calculation of the Thermo-physical Properties of Stainless Steel," *ISIJ International,* vol. 44, no. 10, pp. 1661-1668, 2004.

[9] N. K. Taieh and R. H. A. Abas, "Experimental Study of the Thermal Diffusivity and Heat Capacity Concerning Some Duplex Stainless Steel," *Khwarizmi Engineering Journal,* vol. 11, no. 2, pp. 51-61, 2015.

Acknowledgements